Grafting from versus *grafting to* approaches for the functionalisation of graphene nanoplatelets with poly(methyl methacrylate)

Noelia Rubio,[‡] Heather Au,[‡] Hannah S. Leese, Sheng Hu, Adam J. Clancy and Milo S. P. Shaffer[*]

Department of Chemistry, Imperial College London, London SW7 2AZ, UK.

Keywords: graphene, functionalisation, polymer, grafting from, grafting to, poly(methyl methacrylate)

Accepted: 19th August 2017

*m.shaffer@imperial.ac.uk

‡ Equal contribution

ABSTRACT Graphene nanoplatelets (GNP) were exfoliated using a non-destructive chemical reduction method and subsequently decorated with polymers using two different approaches: *grafting from* and *grafting to*. Poly(methyl methacrylate) (PMMA) with varying molecular weights was covalently attached to the GNP layers using both methods. The grafting ratios were higher (44.6% to 126.5%) for the *grafting from* approach compared to the *grafting to* approach (12.6% to 20.3%). The products were characterised using Thermogravimetric Analysis-Mass Spectrometry (TGA-MS), Raman spectroscopy, X-ray Photoelectron Spectroscopy (XPS), X-Ray Diffraction (XRD), Atomic Force Microscopy (AFM) and Transmission Electron Microscopy (TEM). The g*rafting from* products showed an increase in the grafting ratio and dispersibility in acetone with increasing monomer supply; on the other hand, due to steric effects, the *grafting to* products showed lower absolute grafting ratios and a decreasing trend with increasing polymer molecular weight. The excellent dispersibility of the *grafting from* functionalised graphene, 900 μg/mL in acetone, indicates an increased compatibility with the solvent and the potential to increase graphene reinforcement performance in nanocomposite applications.

Introduction

Graphene related materials are proposed for bulk applications in electronic devices[1], nanocomposites[2-4], supercapacitors[5] and hydrogen storage[6], amongst others. Extensive research

is underway in order to improve the compatibility of graphene with processing solvents and polymeric matrices for the preparation of composites[7, 8]. Covalent functionalisation provides an effective means to adjust the energetics of the surface, as well as to introduce specific steric or electrostatically stabilising moieties. Covalent approaches are more robust than non-covalent alternatives, and avoid any equilibrium with excess free surfactant. These advantages are important in many applications, for example, in the context of composites, where the aim is to enhance the strength of graphene-polymer matrix interfaces. As well as improved compatibility, covalent modification of graphene allows for the stable attachment of groups with specific functional properties (e.g. fluorescent molecules, dopants, etc.)[9,10].

There are several methods in the literature aiming to produce single layer graphene (SLG) from a variety of starting materials (such as few-layer graphenes (FLGs), natural graphite or graphene nanoplatelets (GNPs)). These methods include liquid-phase[11], mechanical[12] or electrochemical exfoliation[13], among others. Graphite Intercalation Compounds (GICs) are established precursors to produce isolated graphene layers with minimal framework damage[14-16]. Exfoliated graphenides can be prepared by various routes, including potassium/liquid ammonia intercalation of graphite[14] and the spontaneous dissolution of potassium-based GICs in N-methyl-2-pyrrolidone (NMP)[17, 18]. Individual charged graphene sheets can be solvated in dry aprotic solvents, and in one recent case, transferred to water[19]. Yet, to stabilise the graphene in other solvents or nanocomposite materials, functional groups are often introduced. The use of covalently grafted polymers is of particular interest for the preparation of nanocomposites[20]. There are two main approaches to prepare polymer-modified carbon nanomaterials (CNMs): *grafting to* and *grafting from*. The *grafting to* method involves the synthesis of a polymer with a reactive end group that is attached to the surface of the CNM. This method allows explicit

control of the molecular weight (M_n) and polydispersity index (PDI). Alternatively, *grafting from* involves *in situ* polymerisation of the monomer directly from the CNM. While the *grafting from* approach promises high grafting ratios, it typically requires the attachment of an initiating group prior to polymerisation[21-23]. *Grafting from* GO (graphite oxide) has been used to grow polystyrene and different methacrylate polymers[22]. These polymers were grown on the surface of GO using radical polymerisation; however, several preparation steps were involved, including the addition of an alkyne molecule to the GO followed by an azide-terminated chain transfer agent, required to initiate polymerisation. Reductive chemistry provides an alternative method that avoids the use of complex initiators. The formation of polymers in GICs was proposed several decades ago in the investigation of the influence of potassium graphite (KC_8) in the "catalysis" of olefin polymerisation[24]. The formation of a "graphite-polymer-composite" was described in 1997 where the compound KC_{24} was prepared from highly oriented pyrolytic graphite (HOPG) and reacted with isoprene or styrene vapour at room temperature[25]. A similar technique was later used in 2006 to produce PMMA-functionalised single-walled nanotubes (SWNTs)[26].

The dispersibility of polymer-functionalised graphene in a specific solvent should be influenced by the amount of grafted polymer and the distribution of the chains on the graphene surface but these factors are poorly understood. The comparison between *grafting from* and *grafting to* approaches has been described for the functionalisation of carbon nanotubes with polystyrene[27], which showed an increase in the dispersibility of the final materials as the grafting ratio increased. A similar study was carried out with graphene oxide[22]; in this case, the authors reported an increase in the grafting ratio when using the *grafting from* approach. Here, we explore how the combination of reductive chemistry and different grafting approaches can

influence the properties of the final product, such as chain length, grafting ratio, and hence solubility. One of the objectives of this work was to maximise the ambient stability of exfoliated graphene layers in organic solvents with minimal framework damage. PMMA was used as both a classic anionic model system and a potentially relevant system in composite applications, for example to increase dispersibility in epoxies[28]. The second objective was to compare *grafting to* and *grafting from* approaches as a function of molecular weight to maximise exfoliation and dispersibility.

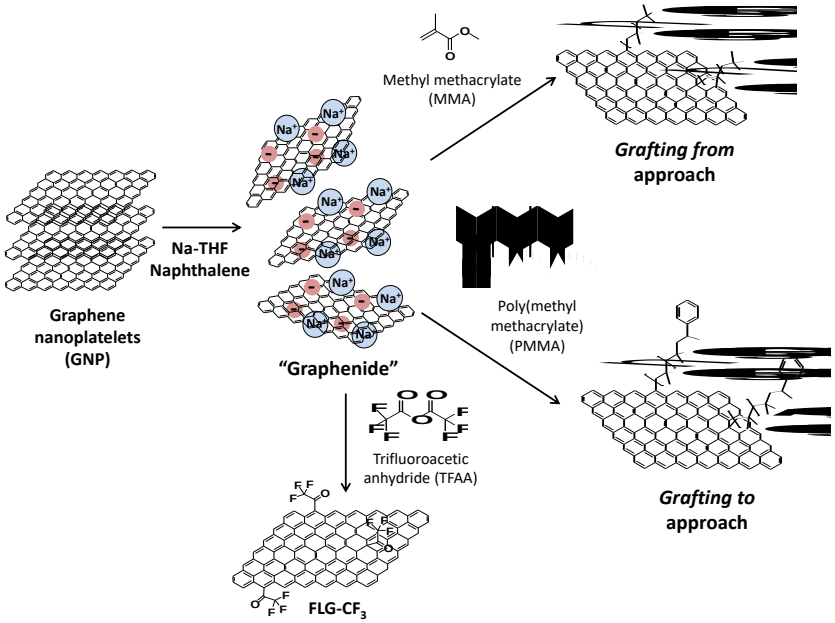

Scheme 1. Grafting methods used for the functionalisation of graphene sheets with PMMA.

Experimental Section

Materials

GNPs were provided by Cambridge Nanosystems UK and used without further purification. 1-Bromododecane, dodecane, copper bromide (I) (CuBr), copper bromide (II) ($CuBr_2$), *N, N*, *N*', *N*'', *N*''-pentamethyldiethylenetriamine (PMDETA), (1-bromoethyl)benzene, glacial acetic acid, sodium (99.95%, ingot), naphthalene (99%), poly(methyl methacrylate), trifluoroacetic anhydride and methyl methacrylate were provided by Sigma-Aldrich UK. Naphthalene was dried under vacuum overnight over phosphorus pentoxide (P_2O_5) before using in the glove box. THF was degassed via a freeze-pump-thaw method and dried over 20 % volume molecular sieves 3 Å before use in the glove box. Methyl methacrylate was previously purified by passing the monomer through an alumina column to remove stabilisers and then degassed using the same method as the THF. CuBr was purified by washing with glacial acetic acid, followed by 2-propanol and stored under nitrogen atmosphere.[29] In order to carry out the ATRP process, acetone and methyl methacrylate were distilled and stored under nitrogen. Immediately before use both monomer and solvent were purged with nitrogen for 30 min. (1-bromoethyl)benzene and PMDETA were used as received. Holey carbon films on 300 mesh copper grids used for TEM experiments were purchased from Elektron Technology UK Ltd. Aluminium oxide 90 active neutral was provided by Merck UK. All gases supplied by BOC, UK.

Polymerisation of PMMA using ATRP

In a typical experiment, CuBr (1.09 mmol, 156.06 mg) and $CuBr_2$ (0.054 mmol, 12.14 mg) were added to a Schlenk flask, equipped with a stirrer bar, which was previously evacuated and flushed with nitrogen. The flask was degassed and filled with nitrogen three times and then left under nitrogen. Subsequently, methyl methacrylate (54.26 mmol, 6 mL) and acetone (3.12 mL) were added to the flask. PMDETA (1.14 mmol, 238.8 μL) was then added to the reaction mixture and the solution was stirred until the Cu complex was formed. The mixture was

degassed using three freeze-pump-thaw cycles. The initiator ((1-bromoethyl)benzene) (1.05 mmol, 149.4 μL) was added after this process and the flask was placed in an oil bath and stirred at 50 °C for different periods of time (30 min, 1 h and 2 h) in order to obtain different molecular weight polymers. The reaction was then stopped by dilution with THF. The solution was filtered through a column filled with neutral aluminium oxide using THF as solvent in order to remove side products. The solvent was evaporated under reduced pressure and the polymer was precipitated in dichloromethane/diethyl ether.

^{1}H-NMR ($CHCl_3$, δ, ppm): 0.77-1.092 (m, 3H, -CH_3), 1.82 (m, 2H, -CH_2-), 3.61 (M, 3H, $COOCH_3$).

GPC (DMF): M_n = 4977 g/mol, Đ = 1.56; M_n = 8039 g/mol, Đ = 1.62 and M_n = 9982 g/mol, Đ = 1.65 for 30 minutes, 1 hour and 2 hours reaction time, respectively

Preparation of sodium naphthalide solution

In a typical experiment, 23 mg (1 mmol) of sodium and 128 mg (1 mmol) of dried naphthalene were dissolved in 10 mL of degassed anhydrous THF in a nitrogen filled glove box, and stirred using a glass stirrer for two hours forming a green sodium-naphthalene solution.

Exfoliated graphene

In a typical experiment, starting material GNP (15 mg) and a glass magnetic bar were placed in a Schlenk tube and flame-dried at 400°C under vacuum. The Schlenk tube was placed in the glove box. 1.04 mL of the sodium naphthalide solution were added to the graphene followed by 11.46 mL of degassed THF (C:Na ratio used was 12, which corresponds to a sodium concentration of 0.01 M).[15] The suspension was stirred for 24 hours. After this period of time, dry N_2/O_2 80/20

was bubbled into the solution for 15 minutes, the solution was stirred for 1 day under N_2/O_2 80/20 vol% for oxidation of any remaining charges on the graphene[15]. Subsequently, the graphene was filtered through a 0.2 μm PTFE filter membrane and washed thoroughly with THF, water and ethanol.

Functionalisation of graphene with trifluoroacetic anhydride (TFAA)

In a typical experiment, starting material GNP (15 mg) and a glass magnetic bar were placed in a Schlenk tube and flame-dried at 400°C under vacuum. The Schlenk tube was placed in the glove box. 1.04 mL of the Na-naphthalene solution were added to the graphene followed by 11.46 mL of degassed THF. The suspension was stirred for 24 hours. After this period of time, the reaction was sealed and transferred outside the glove box and previously degassed TFAA (0.31 mmol, 44.07 μL) were added to the reaction mixture. The solution was allowed to stir for 24 hours. After this period of time, dry N_2/O_2 80/20 vol% was bubbled into the solution for 15 minutes, the solution was stirred for 1 day under N_2/O_2 80/20 for oxidation of any remaining charges on the graphene. The graphene was then filtered through a 0.2 μm PTFE filter membrane and washed thoroughly with THF, water and ethanol.

PMMA functionalised graphene using the *grafting from* approach

In a typical experiment, starting material GNP (15 mg) and a glass magnetic bar were placed in a Schlenk tube and flame-dried at 400°C under vacuum. The Schlenk tube was placed in the glove box. 1.04 mL of the Na-naphthalene solution were added to the graphene followed by 11.46 mL of degassed THF. The suspension was stirred for 24 hours. After this period of time, the reaction

was sealed and transferred outside the glove box and different amounts of previously degassed methyl methacrylate (1.56 mmol, 162 μL (M_n = 800 g/mol), 3.12 mmol, 337 μL (M_n = 1000 g/mol), 6.24 mmol, 674 μL (M_n = 1400 g/mol), 9.36 mmol, 1.035 mL (M_n = 2300 g/mol)) were added to the reaction mixture. The solution was allowed to stir for 24 hours. After this period of time, dry N_2/O_2 80/20 vol% was bubbled into the solution for 15 minutes, the solution was stirred for 1 day under N_2/O_2 80/20 for oxidation of any remaining charges on the graphene. The graphene was then filtered through a 0.2 μm PTFE filter membrane and washed thoroughly with THF, acetone, water and ethanol.

PMMA functionalised graphene using *grafting to* approach

In a typical experiment, starting material GNP (15 mg) and a glass magnetic bar were placed in a Schlenk tube and flame-dried at 400°C under vacuum. The Schlenk tube was placed in the glove box. 1.04 mL of the Na-naphthalene solution (1:1 in THF) were added to the graphene followed by 11.46 mL of degassed THF. The suspension was stirred for 24 hours. After this period of time, different amounts of brominated PMMA (0.104 mmol, 520 mg (M_n = 5000 g/mol), 0.104 mmol, 832 mg (M_n = 8000 g/mol), 0.104 mmol, 1.04 g (M_n = 10000 g/mol)) were added to the reaction mixture. The solution was allowed to stir for 24 hours. After this period of time, dry N_2/O_2 80/20 was bubbled into the solution for 15 minutes, the solution was stirred for 1 day under N_2/O_2 80/20 vol% for oxidation of any remaining charges on the graphene. The graphene was then filtered through a 0.2 μm PTFE filter membrane and washed thoroughly with THF, acetone, water and ethanol.

Measurements

TGA was performed using a METTLER Toledo TGA-DSC 1 integrated with a Hiden HPR–20 QIC EGA mass spectrometer under a N_2 atmosphere. Samples were held at 100°C for 30 min under N_2 flow of 60 ml/min, then ramped at 10°C/min to 800°C. XRD measurements were carried out using dried powder samples. Data were processed using Polymer Labs Cirrus software. These samples were loaded onto zero-background XRD sample holders. The measurement was recorded at a scan rate of 0.108°/s with the Cu Ka (1.542 Å) line using a PANalytical X'Pert PRO diffractometer. Polymer M_n were assessed using a Polymer Labs GPC 50 system with two PL-gel 5 µ columns. Samples were eluted with dimethylformamide (DMF) with 1% triethylamine (TEA) and 1% acetic acid. The instrument was calibrated to PMMA standards. All XPS spectra were recorded using a K-alpha$^+$ XPS spectrometer equipped with a MXR3 Al Kα monochromated X-ray source (hν = 1486.6 eV). X-ray gun power was set to 72 W (6 mA and 12 kV). Charge compensation was achieved using the FG03 flood gun using a combination of low energy electrons and the ion flood source. Argon etching of the samples was done using the standard EX06 Argon ion source using 500 V accelerating voltage and 1 µA ion gun current. Survey scans were acquired using 200 eV pass energy, 1 eV step size and 100 ms (50 ms x 2 scans) dwell times. All high resolution spectra (C1s, and O1s) were acquired using 20 eV pass energy, 0.1 eV step size and 1 second (50ms x 20 scans = 1000 ms) dwell times. Samples were prepared by pressing the sample onto double side sticky carbon based tape. Pressure during the measurement of XPS spectra was $\leq 1 \times 10^{-8}$ mbar. Thermo Avantage software was used for data interpretation. Casa XPS software (version 2.3.16) was used to process the data. The quantification analysis was carried out after subtracting the baseline using the Shirley or two point linear background type. Peaks were fitted using GL(30) lineshapes; a combination of Gaussian (70%) and Lorentzian (30%). All XPS spectra were charge corrected

by referencing the fitted contribution of C-C graphitic like carbon in the C1s signal 284.5 eV. UV-vis-NIR absorption spectra were measured using a Perkin Elmer Lambda 950 UV-vis spectrometer in the range of wavelengths between 800 and 400 nm. A quartz cuvette with 1 cm pathlength was used for these measurements. Raman spectra of powder samples were measured using a Renishaw in Via confocal Raman spectrometer equipped with a 532 nm excitation laser source; mapping measurements were carried out using the Streamline mode (between 500 – 1000 spectra over at least 3 different areas). Samples were prepared by drop casting graphene dispersions on a glass slide. The exposure time was 10 s with a laser intensity of 3.2 mW and grating 1800 l/mm. Data were analysed using Wire 4.1 and OriginPro 9. The D peak was fitted by one Gaussian function, and the G and 2D peaks were fitted using a mixture of Lorentz and Gaussian functions. Tapping-mode atomic force microscopy (AFM) measurements were taken using Bruker MultiMode 8 AFM. Samples for AFM were prepared by drop-casting dilute dispersed-graphene chloroform solutions on silica substrates. ^{1}H-NMR measurements were carried out using a Bruker NM 400 spectrometer operating at 9.4 T. Samples were dissolved in Deuterated chloroform ($CDCl_3$) and all spectra were recorded with 16 scans. All chemical shifts (δ) are given in ppm, where the residual $CHCl_3$ peak was used as an internal reference (δ = 7.28 ppm). TEM was carried out using a JEOL2100Plus TEM at 200 kV operating voltage. One drop of the graphene solution in acetone (100 μg/mL) was deposited on a TEM grid and allowed to evaporate at room temperature. The TEM grid was subsequently kept under vacuum overnight before the measurement. The measurements of adsorption and desorption isotherms of nitrogen at 77 K were carried out on 20 mg-50 mg of FLG using a Micromeritics ASAP 2010 apparatus. Specific surface areas were calculated according to the Brunauer, Emmett and Teller (BET)

equation from the adsorption isotherms in the relative pressure range of 0.05 p/p0–0.20 p/p0. Prior to analysis, the samples were degassed with continuous N_2 flow at 100 °C for 12 hours.

Results and discussion

The selected starting material was a type of GNP grown by chemical vapour deposition (CVD); it provides a relatively crystalline framework by a simple one step synthesis, whilst offering high exfoliation yields in subsequent reactions. The exfoliation of the GNP starting material was carried out using a standard methodology developed for grafting short alkyl groups[15, 30]: sodium and naphthalene were used as the reducing agent and transfer reagent (**Scheme 1**), respectively. Tetrahydrofuran (THF) was used as the solvent due to its ability to coordinate sodium ions[31]. PMMA was grafted from the graphenide by adding methyl methacrylate (MMA) monomer to the chemically reduced graphene solution. GNP was exfoliated into FLG using a C/sodium ratio of 12 reported previously[15], based on an optimum value found to balance the need to charge the graphenide with the tendency for charge condensation. Sodium/MMA ratios of 1:15, 1:30, 1:60 and 1:90 were used in order to grow polymers of different molecular weights. The resulting GNP-PMMA products were characterised using TGA-MS under nitrogen. The GNP starting material shows a small mass loss (2.8 wt%) in the range from 100 °C to 800 °C (**Figure S1A**), probably due to the decomposition of organic impurities or oxygen functionalities, while the exfoliated sample (Na-reduced FLG) shows a mass loss (13.8 wt%) related to the presence of THF molecules in the sample (m/z = 41, **Figure S1B**). TGA-MS of PMMA-grafted FLG samples prepared using the *grafting from* approach (**Figure 1A** top panel) show the expected PMMA fragments (m/z = 69 and m/z = 100) evolved in the same temperature range on which

pure PMMA homopolymer fully decomposes (**Figure S3**). However, the m/z = 41 peak indicates the presence of some solvent molecules within the graphene layers after the reaction, suggesting the formation of stage-1 Na-THF-GICs complexes[15, 31]. In order to quantify the ratio of trapped solvent and grafted PMMA on the graphene layers, the relative mass fractions of each component were estimated from the MS peaks (**Figure S2** and **Table S1** for more details). Controls were prepared by mixing either MMA or PMMA-Br (M_n ~ 5000 g/mol) with quenched Na-reduced FLG (ESI); in both cases, TGA-MS after work-up (**Figure S6A-B**) showed no MMA-related signals, ruling out physisorption of either monomer or polymer. Grafting ratio is defined as the weight percentage of covalently attached polymer relative to the graphitic carbon. High grafting ratios were obtained using the *grafting from* approach (44.6% - 126.5%, **Table 1**). There are actually a number of active sites which are expected to be determined by the number of charges and is only a fraction of the total charge introduced[32, 33]. In order to estimate the number of active sites initiating the polymerisation, the graphenide was functionalised with trifluoroacetic anhydride (TFAA) (**Scheme 1**). This molecule is a similar size and contains a trifluoromethyl group that can be detected using TGA-MS and XPS; whilst the reactivities of TFAA and MMA may not be the identical, any variation will generate only a relative shift of otherwise consistent grafting trends. Both techniques (**Figure S5**) quantified the fluorine-containing groups grafted on the layers (one group every 149 carbon atoms from XPS calculations), and hence indicate the efficiency of the grafting reaction (**Table S2**). Raman spectroscopy (**Figure S5**) also confirmed the introduction of these functional groups. The M_n of the grafted polymer was estimated from the grafting ratio, by assuming the same density of active sites (**Table S1**). The values varied from 800 g/mol up to 2300 g/mol, increasing as expected with MMA:Na ratio.

Bromine-terminated PMMA polymers with different M_n were prepared for the *grafting to* approach, using Atom Transfer Radical Polymerisation (ATRP), following a previous protocol[29]. The polymerisation process was carried out varying the reaction times in order to obtain polymers with different M_n in the range from 5000 to 10000 g/mol. As noted above, a simple mixing control excludes possible physisorption. The negative charges on the graphene surface react with the bromine-terminated polymer (electrophile), to form the products FLG-*g*-*t* 5000, FLG-*g*-*t* 8000 and FLG-*g*-*t* 10000. TGA-MS analysis (**Figure 1A** bottom panel) shows typical PMMA fragments for all the grafted samples (m/z = 69 and m/z = 100). Mass loss values were extracted from the TGA graphs taking into account the amount of trapped solvent (**Table 1**). Grafting ratio decreases as the M_n of the grafted polymer increases (from 20.3% down to 12.6%, for FLG-*g*-*t* 5000 and FLG-*g*-*t* 10000, respectively), likely due to increased steric hindrance as discussed.

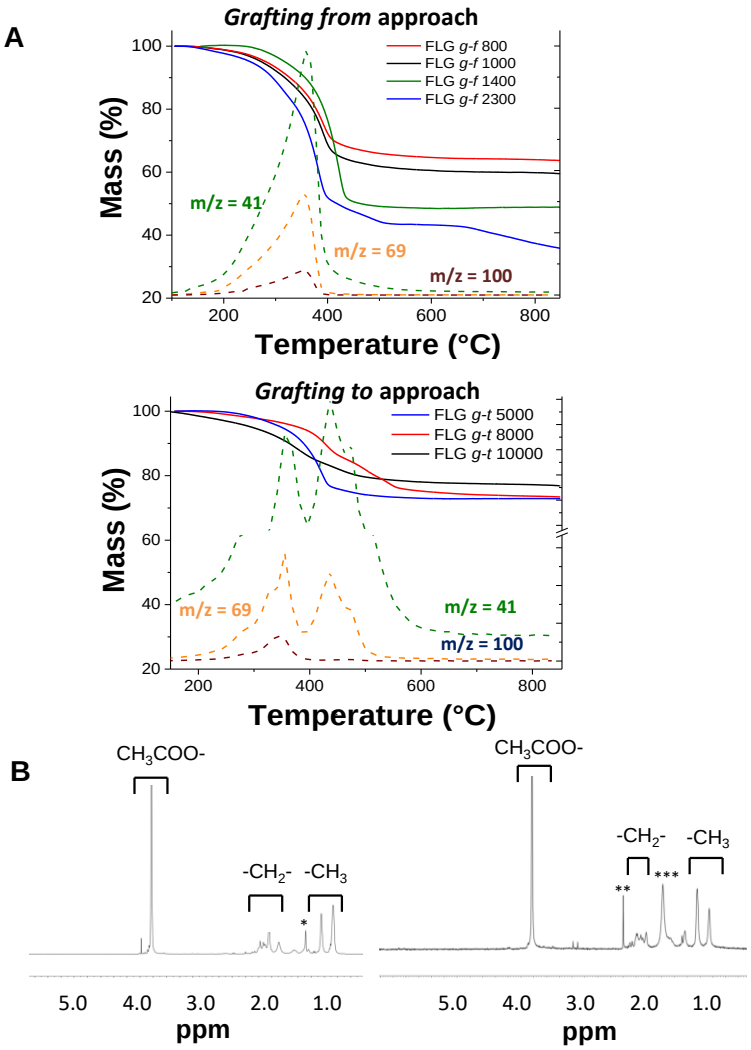

Figure 1. Characterisation of PMMA-grafted GNP. (A) TGA-MS of the PMMA-grafted GNP using *grafting from* (top panel) and *grafting to* approaches (bottom panel). MS fragments correspond to CH_2=CH-CH_2^+ (m/z = 41), CH_2=C=C-O-CH_3^+ (m/z= 69) and CH_2=CH-CO-O-CH_3^+ (m/z = 100). (B) ^{1}H-NMR spectra of commercial PMMA polymer (left panel) and FLG-*g-f* 1400 (right panel).*, ** and *** indicate the presence of residual tetrahydrofuran, acetone and water, respectively.

The ^{1}H-NMR spectrum of commercial PMMA shows the typical signals from the polymer (**Figure 1B** left panel). The peak at 3.6 ppm corresponds to the protons from $COOCH_3$ in each

MMA unit. The peaks observed at 0.89 ppm and 1.09 ppm correspond to the CH_3 groups, while the peaks at 1.57 ppm are attributed to the CH_2 groups. These peaks can be observed in the spectrum from FLG-*g-f* 1400 (**Figure 1B** right panel), confirming the presence of polymer on the graphene layers. Polymer signals were also observed for the sample FLG-*g-f* 2300 (**Figure S7**); however, these signals were very weak for the sample FLG-*g-f* 1000, probably due to the lower polymer content and hence, dispersibility (see below). Similarly, measurable NMR peaks were weaker for the *grafting to* samples.

Raman spectroscopy provided quantitative data about the ratios of the D and G bands and 2D and G bands obtained from statistical mapping experiments (I_D/I_G and I_{2D}/I_G respectively) (**Figure 2**). Mean I_D/I_G values of 0.52 ± 0.02 for the *grafting from* approach showed an increase compared to the GNP starting material (I_D/I_G 0.40 ± 0.02**, Figure S8A**), suggesting an increase in the number of sp^3 atoms due to the presence of grafting sites after the polymerisation process. The much lower I_D/I_G values of 0.42±0.03 displayed by the *grafting to* products are not significantly greater than the Na-reduced control sample. This result is not surprising since the grafting density for the *grafting to* approach is an order of magnitude lower compared to the *grafting from* approach (**Table 1**), due to the steric bulk of the polymers. The ratio of the 2D band and G band (I_{2D}/I_G) averages 0.49 ± 0.03 for GNP starting material; an increase in this ratio indicates the presence of a higher proportion of SLG in the sample. A value of I_{2D}/I_G up to 0.59 ± 0.04 was observed for the Na-reduced FLG (**Figure S8B**), suggesting an increase in the degree of exfoliation. Higher I_{2D}/I_G ratios for PMMA grafted samples indicate greater exfoliation of the graphene layers after the functionalization. This increase in the I_{2D}/I_G ratios was larger for the *grafting from* approach (up to 0.77 ± 0.05) compared to the *grafting to* approach (0.62 ± 0.02). These samples show a high intensity and symmetrical 2D band, this shape suggests the existence

of single-layer and/or few layer graphene[34]. The full width at half maximum of the 2D band ($FWHM_{2D}$) did not change significantly between samples (**Table S5**), and is typical of chemically exfoliated FLG[35].

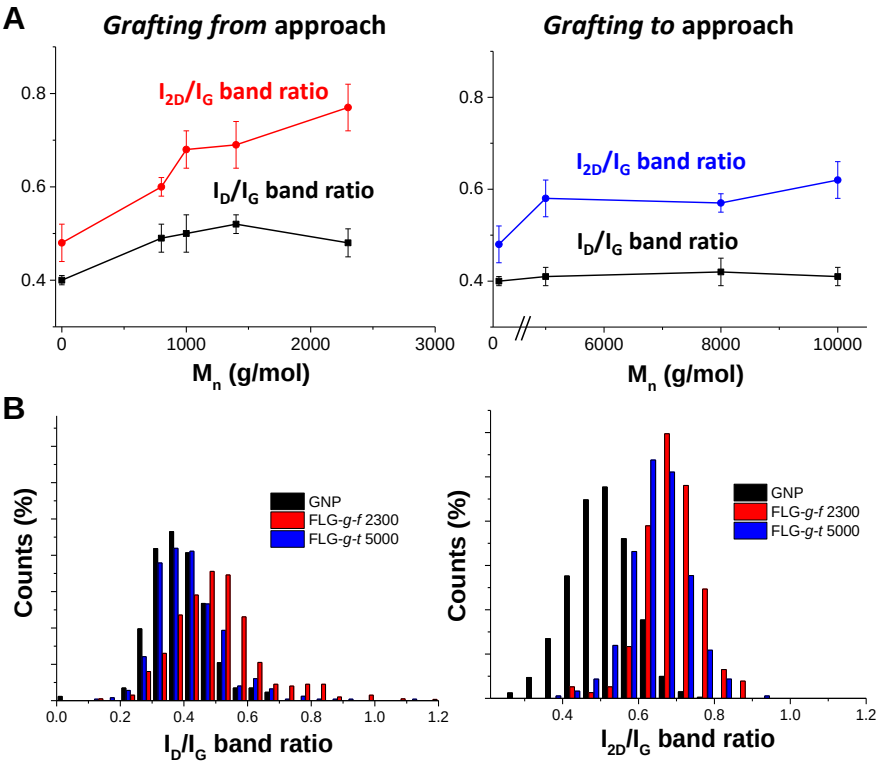

Figure 2. (A) Average I_D/I_G and I_{2D}/I_G ratios of FLG-PMMA obtained using *grafting from* and *grafting to* approaches and (B) I_D/I_G and I_{2D}/I_G histograms of FLG-*g*-*f* 2300 and FLG-*f*-*t* 5000 representative samples of both approaches.

C1s XPS spectra of Na-reduced FLG, FLG-*g*-*f* 2800 and FLG-*g*-*t* 5000 samples (**Figure 3A**) were deconvoluted into different bands: C=C and C-C (284.5 eV), C-O and C=O (286.4 eV), COOR (288.7 eV) and the π-π* transition (290.7 eV) (See **Table 1** for quantitative data of all the samples). Similar components are observed for Na-reduced FLG and for the GNP starting material (**Figure S9**), suggesting that the exfoliation process does not itself introduce a large

number of additional oxygen functionalities on the graphene layers. The slight increase in the absolute amount of oxygen after the exfoliation process (from 4% to 5%) could be due to the presence of trapped solvent within the layers (**Table 1**). On the other hand, when carrying out the reaction using the *grafting from* and *grafting to* approaches, a significant increase in the COO- band appears, together with a broadening of the C=C/C-C band due to an increase in the number of C-C bonds and a higher contribution from the C=O band. The oxygen and carbon atomic percentages change very significantly after introducing the different polymers (**Table 1**). FLG-*g*-*f* 2300 has an oxygen content of 23.5% while FLG-*g*-*t* 5000 sample shows a lower value of 9.58%, consistent with a lower degree of functionalisation for the *grafting to* approach. The grafting density (expressed as number of graphene carbon atoms per polymer chain) obtained from XPS values is in good agreement with the results obtained from TGA values, after subtracting the excess solvent still trapped within the graphene layers (**Table 1**). For the samples obtained using the *grafting from* approach, the grafting density found from XPS varied between 150 and 340, which is close to the value obtained from TGA calculations (one functional group every 149 carbon atoms). The low sodium content found in the samples (0.11% ± 0.02%) indicates that the majority of the metal used for the exfoliation was removed by washing. Deconvolution of the O1s spectrum (**Figure 3B**) results in two different peaks, O-C (532.05 eV) and O=C (533.4 eV), related to PMMA, which are similar for the grafted samples.

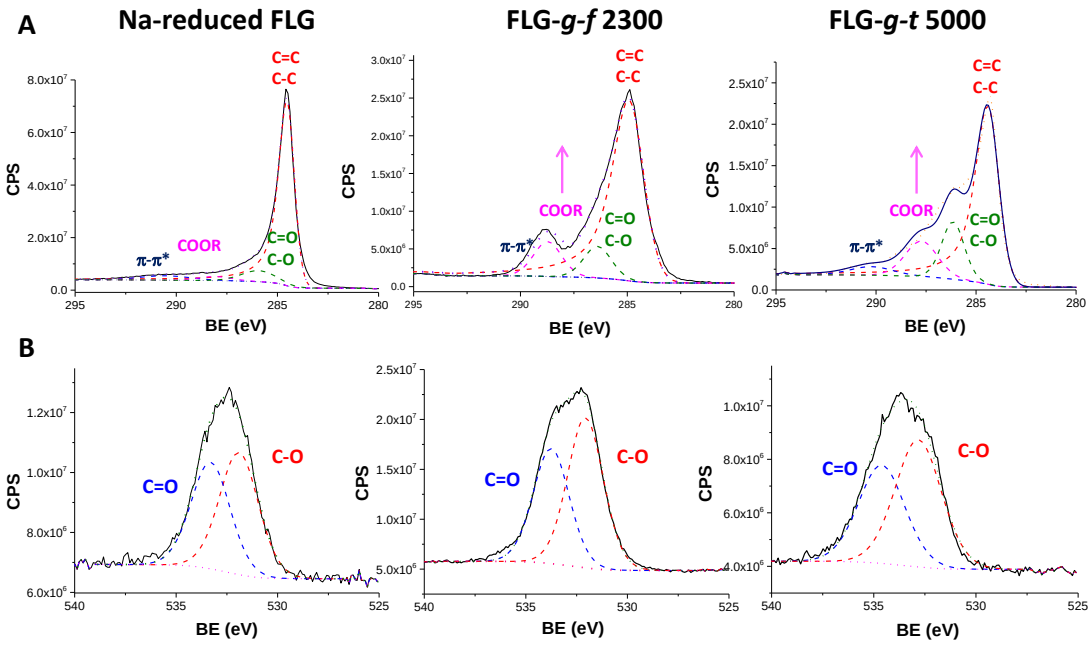

Figure 3. Deconvoluted XPS spectra of the (A) C1s and (B) O1s regions obtained from Na-reduced FLG (left panels), FLG-*g-f* 2300 (middle panels) and FLG-*g-t* 5000 (right panels). These samples were chosen as representative examples of both grafting approaches.

XRD measurements provide information about the interlayer distance (d) using Bragg's law and the number of stacked layers (N) using the Scherrer equation[36]. X-ray diffractograms (**Figure S10**) of the different graphene-polymer samples show the typical graphite (002) peak at a 2θ value of 26.2°. The weak diffraction pattern of the GNP starting material (**Figure S10**, left panel) suggests that the graphene layers of the initial material are partially exfoliated. After the polymerisation process, a broadening of the (002) peak is observed for all samples, indicating successful further exfoliation of the FLG material[37]. The average number of layers was 41 for the GNP starting material (**Table S6**) and 16 for the Na-reduced FLG. After functionalisation with PMMA, the number of layers per stack decreased to an average of 6 and 9 layers for the *grafting from* and *grafting to* method, respectively.

The morphology and degree of exfoliation of the FLG-PMMA were assessed using Atomic Force Microscopy (AFM) and Transmission Electron Microscopy (TEM) (**Figure 4**). AFM images of GNP starting material show agglomerated flakes with heights between 20.6 ± 5.5 nm, corresponding to an average of 61 layers. Na-reduced FLG shows a lateral size of 639.9 nm ± 171.4 nm. The presence of few-layer graphene in this sample indicates successful exfoliation of the starting material (average height: 4.4 nm ± 0.61nm). FLG-*g-f* 2300 shows a better degree of exfoliation, the average height in this case is 3.1 nm ± 0.4 nm, in good agreement with the results obtained from XRD measurements; the average number of layers significantly decreased after functionalisation with PMMA.

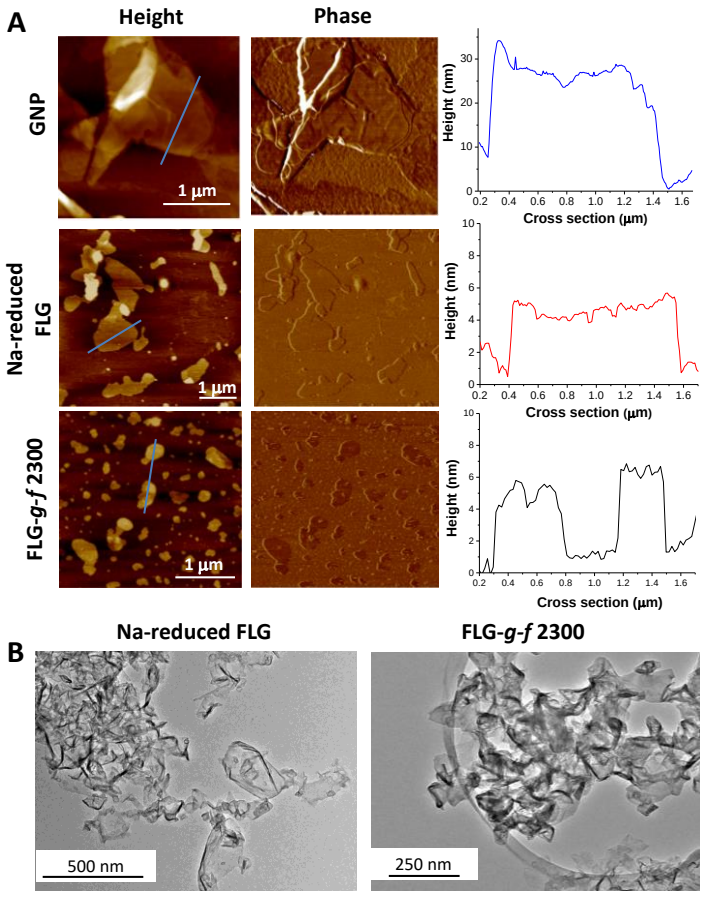

Figure 4. AFM images (A) of GNP starting material, Na-reduced FLG and FLG-*g-f* 2300. TEM images (B) Na-reduced FLG and FLG-*g-f* 2300.

Table 1. Summary of grafting analysis data for FLG-PMMA samples

Sample	Grafting ratio (%)	Dispersibility (mg/mL)	Grafting density[a]	Grafting density[b]	C (%)[b]	O (%)[b]	Surface concentration of grafted PMMA (μmol m^{-2})[a]	PMMA separation *D* (nm)	R_F (nm)
GNP	-	3.8	-	-	95.9	3.91	-	-	-
Na-reduced FLG	-	530	-	-	94.3	5.22	-	-	-
FLG-*g-f* 800	44.6	720	149	278	89.7	9.9	0.85	1.6	1.8
FLG-*g-f* 1000	55.6	760	149	334	89.2	10.1	0.80	1.6	2.1
FLG-*g-f* 1400	79.1	875	149	151	79.6	20.2	0.65	1.8	2.6
FLG-*g-f* 2300	126.5	920	149	208	75.6	23.5	0.50	2.1	5.0
FLG-*g-t* 5000	20.3	670	2055	1869	89.7	10.0	0.07	5.5	5.8
FLG-*g-t* 8000	15.1	650	4421	4390	90.9	9.0	0.03	8.0	7.7
FLG-*g-t* 10000	12.6	710	6615	5490	91.6	8.2	0.02	9.5	8.8

[a] Values obtained from TGA calculations. [b] Values obtained from XPS calculations.

TEM images (**Figure 4B**) of Na-reduced FLG and FLG-*g-f* 2800 show a similar morphology to the starting material (**Figure S11**), suggesting that the exfoliation/functionalisation procedure did not damage the graphene sheets. The lateral sizes for individual graphene sheets are in the range between 200 and 500 nm, with no significant differences observed after functionalisation.

Overall, the TGA-MS and XPS data indicate that PMMA polymer was successfully introduced on the graphene surface by both *grafting from* and *grafting to* methods. Both the grafting ratio and the grafting density were higher for the *graft from* reactions (**Table 1**). Raman and XRD data suggest that a much greater degree of exfoliation was achieved by the *grafting from* method, which is also supported by AFM observations.

The grafting ratio trend of the *grafting from* products shows an increase from 44.6% (FLG-*g-f* 1100) up to 126.5% (FLG-*g-f* 2300) as the M_n increases (**Figure 5A**); a similar trend was reported, for the functionalisaton of carbon nanotubes with polystyrene grown by ATRP[27]. However, the estimated M_n values obtained for the FLG-*g-f* products were lower than reported

for the ring opening polymerisation of caprolactam on oxidised carbon nanotubes[38] (estimated 1280 - 8480 g/mol). On the other hand, the *grafting to* products show the opposite trend in grafting ratios, compared to the *grafting from* approach (**Figure 5A**), most likely due to steric hindrance. Once a polymer chain grafts on the graphene surface, its volume occludes a large area of that surface, preventing grafting of another chain nearby. The grafting ratio of polystyrene-grafted to SWNTs was also reported to decrease with M_n[39]. For each of the FLG products, the surface concentration of grafted polymer and average PMMA chain separation, *D,* were estimated using the Na-reduced FLG specific surface area (420.08 $m^2/g \pm 4.51$ m^2/g) (**Table 1** and **Table S5**)[30]. The conformation of the grafted PMMA polymer can be predicted from the average separation, *D,* between grafting sites. The estimated spacings ranged between 1.6 and 2.1 nm for the *grafting from* products; this value is below the theoretical values of the Flory radius (obtained using $R_F = M^{3/5}a$, where *a* is the repeat length and *M* the number of monomers per chain)[40] for all the samples. According to de Gennes' model[40], this trend suggests that the polymers must therefore grow in a brush-like fashion. Adjusting the estimates to account for the observed degree of exfoliation does not change the expected conformation (see ESI for more information). The *grafting to* approach shows *D* values in the range between 5.5 nm and 9.5 nm for polymer chains between 5000 and 10000 g/mol. These values are similar to or larger than the calculated R_F values (between 5.8 nm and 8.8 nm), suggesting that the polymer follows a mushroom regime in this case, where the polymer chains coil. These changes in regime are consistent with the grafting ratio trends and the proposed mechanisms.

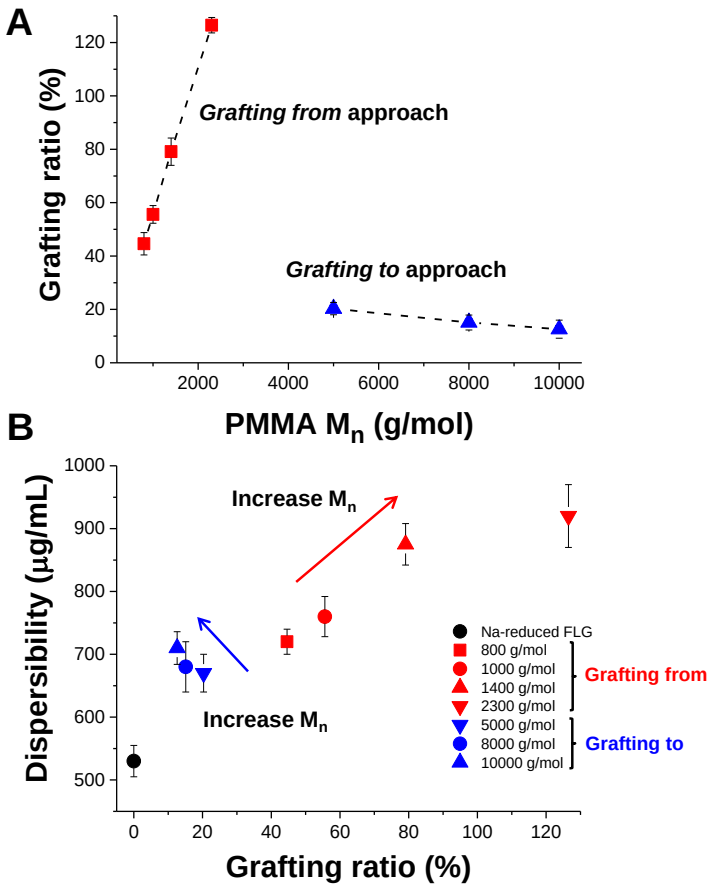

393

394 **Figure 5.** Grafting density and dispersibility plots of PMMA grafted FLG using the *grafting*

395 *from* and *grafting to* approaches.

396 The dispersibility of PMMA-grafted FLG in acetone was quantified using UV-vis spectroscopy.

397 A known mass was sonicated in acetone for five minutes, allowed to sediment overnight, and the

398 supernatant concentrations measured using the extinction coefficient[11] of graphene in solution

399 (α_{660} = 2460 L/g m). The dispersibility of GNP starting material was low (3.8 µg/ml) (**Figure**

400 **S12**) but increased remarkably for Na-reduced FLG (530 µg/ml) and polymer modified

401 graphene, by 250 times for FLG-*g*-*f* 1400 (920 µg/ml) and 170 times for FLG-*g*-*t* 5000 (650

402 µg/ml). The trend according to the grafting ratios shows an increase in the dispersibility of the

403 material as the grafting ratio increases for the *grafting from* approach (**Figure 5** bottom panel).

On the other hand, the dispersibility behaviour remained the same for the different materials obtained from the *grafting to* approach. These values are higher than values reported in the literature for reduced-GO-PMMA with different M_n polymers attached to the graphene layers, 150 μg/ml and 140 μg/ml for graphene-PMMA *g-f* 10000 and graphene-PMMA *g-t* 5000, respectively,[22] with grafting ratios of 49.3% and 50.7%, respectively. Improved grafting ratio and dispersibility results in the present study are very promising for the incorporation of PMMA-grafted FLG into different matrices.

Conclusion

In conclusion, reductive chemistry provides a route to functionalise graphene with PMMA polymers via both *grafting to* and *grafting from* approaches. Direct anionic polymerisation using graphenide as an initiator was particularly effective for grafting PMMA in situ, without the need of introducing specific initiator groups. The grafting ratio was high and systematically controlled by monomer addition. The solubility in acetone of the *grafting from* products is directly related to the M_n and grafting ratios (**Figure 5**), with an increase in the solubility when increasing M_n; however, it is not straight forward to measure the M_n of the polymer attached on the surface of the graphene. On the other hand, while there is perfect control of the polymer M_n when using the *grafting to* approach, the solubility and grafting ratios obtained are lower compared to the *grafting from* approach. The use of reductive chemistry for *in situ* polymerization should allow the introduction of block polymers and other variants in the future. This approach should also be applicable to a range of graphitic starting materials including natural graphite, synthetic graphite or FLG. The final polymer-graphene hybrids could be used in a wide range of applications, such as sensors, as electrodes in energy storage materials, biomedical materials and in coatings for fuselages.

ASSOCIATED CONTENT

Data statement

Supporting data can be requested from the corresponding author, but may be subject to confidentiality obligations.

AUTHOR INFORMATION

Corresponding Author

*m.shaffer@imperial.ac.uk

Author Contributions

‡ Equal contribution

Notes

The authors declare no competing financial interests.

ACKNOWLEDGMENT

We are grateful to Dr. Ignacio Villar-García (Imperial College London) for discussions in interpreting XPS spectra. Funding from Engineering and Physical Sciences Research Council (EPSRC/EP/K016792/1 and EP/K01658X/1) is also acknowledged. We are also grateful to Catharina Paukner (FGV Cambridge Nanosystems Limited) for providing the GNP starting material.

448 REFERENCES

449 1. Zhang, J. S.; Chen, Y.; Wang, X. C. Two-dimensional covalent carbon nitride
450 nanosheets: synthesis, functionalization, and applications. *Energ Environ Sci* **2015,** 8 (11), 3092-
451 3108 DOI: 10.1039/c5ee01895a.
452 2. Wang, F. Z.; Drzal, L. T.; Qin, Y.; Huang, Z. X. Mechanical properties and thermal
453 conductivity of graphene nanoplatelet/epoxy composites. *J Mater Sci* **2015,** 50 (3), 1082-1093
454 DOI: 10.1007/s10853-014-8665-6.
455 3. Das, B.; Eswar Prasad, K.; Ramamurty, U.; Rao, C. N. Nano-indentation studies on
456 polymer matrix composites reinforced by few-layer graphene. *Nanotechnology* **2009,** 20 (12),
457 125705 DOI: 10.1088/0957-4484/20/12/125705.
458 4. Jung, H.; Yu, S.; Bae, N. S.; Cho, S. M.; Kim, R. H.; Cho, S. H.; Hwang, I.; Jeong, B.;
459 Ryu, J. S.; Hwang, J.; Hong, S. M.; Koo, C. M.; Park, C. High through-plane thermal conduction
460 of graphene nanoflake filled polymer composites melt-processed in an L-shape kinked tube. *ACS*
461 *applied materials & interfaces* **2015,** 7 (28), 15256-62 DOI: 10.1021/acsami.5b02681.
462 5. Liu, C. G.; Yu, Z. N.; Neff, D.; Zhamu, A.; Jang, B. Z. Graphene-Based Supercapacitor
463 with an Ultrahigh Energy Density. *Nano Lett* **2010,** 10 (12), 4863-4868 DOI:
464 10.1021/nl102661q.
465 6. Tozzini, V.; Pellegrini, V. Prospects for hydrogen storage in graphene. *Phys Chem Chem*
466 *Phys* **2013,** 15 (1), 80-89 DOI: 10.1039/c2cp42538f.
467 7. Ahmadi-Moghadam, B.; Sharafimasooleh, M.; Shadlou, S.; Taheri, F. Effect of
468 functionalization of graphene nanoplatelets on the mechanical response of graphene/epoxy
469 composites. *Mater Design* **2015,** 66, 142-149 DOI: 10.1016/j.matdes.2014.10.047.
470 8. Tang, L. C.; Wan, Y. J.; Yan, D.; Pei, Y. B.; Zhao, L.; Li, Y. B.; Wu, L. B.; Jiang, J. X.;
471 Lai, G. Q. The effect of graphene dispersion on the mechanical properties of graphene/epoxy
472 composites. *Carbon* **2013,** 60, 16-27 DOI: 10.1016/j.carbon.2013.03.050.
473 9. Gatti, T.; Vicentini, N.; Mba, M.; Menna, E. Organic Functionalized Carbon
474 Nanostructures for Functional Polymer-Based Nanocomposites. *Eur J Org Chem* **2016,** (6),
475 1071-1090 DOI: 10.1002/ejoc.201501411.
476 10. Liu, J. W.; Ye, Y. S.; Xue, Y.; Xie, X. L.; Mai, Y. W. Recent Advances in Covalent
477 Functionalization of Carbon Nanomaterials with Polymers: Strategies and Perspectives. *J Polym*
478 *Sci Pol Chem* **2017,** 55 (4), 622-631 DOI: 10.1002/pola.28426.
479 11. Hernandez, Y.; Nicolosi, V.; Lotya, M.; Blighe, F. M.; Sun, Z. Y.; De, S.; McGovern, I.
480 T.; Holland, B.; Byrne, M.; Gun'ko, Y. K.; Boland, J. J.; Niraj, P.; Duesberg, G.; Krishnamurthy,
481 S.; Goodhue, R.; Hutchison, J.; Scardaci, V.; Ferrari, A. C.; Coleman, J. N. High-yield
482 production of graphene by liquid-phase exfoliation of graphite. *Nat Nanotechnol* **2008,** 3 (9),
483 563-568 DOI: 10.1038/nnano.2008.215.
484 12. Leon, V.; Rodriguez, A. M.; Prieto, P.; Prato, M.; Vazquez, E. Exfoliation of Graphite
485 with Triazine Derivatives under Ball-Milling Conditions: Preparation of Few-Layer Graphene
486 via Selective Noncovalent Interactions. *Acs Nano* **2014,** 8 (1), 563-571 DOI: 10.1021/nn405148t.
487 13. Zhou, M.; Tang, J.; Cheng, Q.; Xu, G. J.; Cui, P.; Qin, L. C. Few-layer graphene obtained
488 by electrochemical exfoliation of graphite cathode. *Chem Phys Lett* **2013,** 572, 61-65 DOI:
489 10.1016/j.cplett.2013.04.013.
490 14. Milner, E. M.; Skipper, N. T.; Howard, C. A.; Shaffer, M. S. P.; Buckley, D. J.; Rahnejat,
491 K. A.; Cullen, P. L.; Heenan, R. K.; Lindner, P.; Schweins, R. Structure and Morphology of

Charged Graphene Platelets in Solution by Small-Angle Neutron Scattering. *J Am Chem Soc* **2012,** 134 (20), 8302-8305 DOI: 10.1021/ja211869u.
15. Morishita, T.; Clancy, A. J.; Shaffer, M. S. P. Optimised exfoliation conditions enhance isolation and solubility of grafted graphenes from graphite intercalation compounds. *J Mater Chem A* **2014,** 2 (36), 15022-15028 DOI: 10.1039/c4ta02349h.
16. Penicaud, A.; Drummond, C. Deconstructing Graphite: Graphenide Solutions. *Accounts Chem Res* **2013,** 46 (1), 129-137.
17. Valles, C.; Drummond, C.; Saadaoui, H.; Furtado, C. A.; He, M.; Roubeau, O.; Ortolani, L.; Monthioux, M.; Penicaud, A. Solutions of Negatively Charged Graphene Sheets and Ribbons. *J Am Chem Soc* **2008,** 130 (47), 15802-+ DOI: 10.1021/ja808001a.
18. Catheline, A.; Valles, C.; Drummond, C.; Ortolani, L.; Morandi, V.; Marcaccio, M.; Iurlo, M.; Paolucci, F.; Penicaud, A. Graphene solutions. *Chem Commun* **2011,** 47 (19), 5470-5472 DOI: 10.1039/c1cc11100k.
19. Bepete, G.; Anglaret, E.; Ortolani, L.; Morandi, V.; Huang, K.; Penicaud, A.; Drummond, C. Surfactant-free single-layer graphene in water. *Nat Chem* **2017,** 9 (4), 347-352 DOI: 10.1038/Nchem.2669.
20. Raji, A. R. O.; Varadhachary, T.; Nan, K. W.; Wang, T.; Lin, J.; Ji, Y. S.; Genorio, B.; Zhu, Y.; Kittrell, C.; Tour, J. M. Composites of Graphene Nanoribbon Stacks and Epoxy for Joule Heating and Deicing of Surfaces. *ACS applied materials & interfaces* **2016,** 8 (5), 3551-3556 DOI: 10.1021/acsami.5b11131.
21. Fang, M.; Wang, K. G.; Lu, H. B.; Yang, Y. L.; Nutt, S. Single-layer graphene nanosheets with controlled grafting of polymer chains. *J Mater Chem* **2010,** 20 (10), 1982-1992 DOI: 10.1039/b919078c.
22. Ye, Y. S.; Chen, Y. N.; Wang, J. S.; Rick, J.; Huang, Y. J.; Chang, F. C.; Hwang, B. J. Versatile Grafting Approaches to Functionalizing Individually Dispersed Graphene Nanosheets Using RAFT Polymerization and Click Chemistry. *Chem Mater* **2012,** 24 (15), 2987-2997 DOI: 10.1021/cm301345r.
23. Choi, J. H.; Oh, S. B.; Chang, J. H.; Kim, I.; Ha, C. S.; Kim, B. G.; Han, J. H.; Joo, S. W.; Kim, G. H.; Paik, H. J. Graft polymerization of styrene from single-walled carbon nanotube using atom transfer radical polymerization. *Polym Bull* **2005,** 55 (3), 173-179 DOI: 10.1007/s00289-005-0426-x.
24. Podall, H. F., W.E.; Giraitis, A.P. Catalytic Graphite Inclusion Compounds. I. Potassium Graphite as a Polymerization Catalyst. *The Journal of Organic Chemistry* **1958,** 23 (1), 82-85.
25. Shioyama, H. Polymerization of isoprene and styrene in the interlayer spacing of graphite. *Carbon* **1997,** 35 (10-11), 1664-1665 DOI: Doi 10.1016/S0008-6223(97)82797-2.
26. Liang, F.; Beach, J. M.; Kobashi, K.; Sadana, A. K.; Vega-Cantu, Y. I.; Tour, J. M.; Billups, W. E. In situ polymerization initiated by single-walled carbon nanotube salts. *Chem Mater* **2006,** 18 (20), 4764-4767 DOI: 10.1021/cm0607536.
27. Qin, S. H.; Qin, D. Q.; Ford, W. T.; Resasco, D. E.; Herrera, J. E. Functionalization of single-walled carbon nanotubes with polystyrene via grafting to and grafting from methods. *Macromolecules* **2004,** 37 (3), 752-757 DOI: 10.1021/ma035214q.
28. Gomez, C. M.; Bucknall, C. B. Blends of Poly(Methyl Methacrylate) with Epoxy-Resin and an Aliphatic Amine Hardener. *Polymer* **1993,** 34 (10), 2111-2117 DOI: Doi 10.1016/0032-3861(93)90737-U.

29. Sarbu, T.; Lin, K. Y.; Ell, J.; Siegwart, D. J.; Spanswick, J.; Matyjaszewski, K. Polystyrene with designed molecular weight distribution by atom transfer radical coupling. *Macromolecules* **2004,** 37 (9), 3120-3127 DOI: 10.1021/ma035901h.
30. Leese, H. S.; Govada, L.; Saridakis, E.; Khurshid, S.; Menzel, R.; Morishita, T.; Clancy, A. J.; White, E. R.; Chayen, N. E.; Shaffer, M. S. P. Reductively PEGylated carbon nanomaterials and their use to nucleate 3D protein crystals: a comparison of dimensionality. *Chemical Science* **2016**, DOI: 10.1039/C5SC03595C.
31. Inagaki, M.; Tanaike, O. Host Effect on the Formation of Sodium-Tetrahydrofuran-Graphite Intercalation Compounds. *Synthetic Met* **1995,** 73 (1), 77-81 DOI: Doi 10.1016/0379-6779(95)03300-9.
32. Hodge, S. A.; Tay, H. H.; Anthony, D. B.; Menzel, R.; Buckley, D. J.; Cullen, P. L.; Skipper, N. T.; Howard, C. A.; Shaffer, M. S. P. Probing the charging mechanisms of carbon nanomaterial polyelectrolytes. *Faraday Discuss* **2014,** 172, 311-325 DOI: 10.1039/c4fd00043a.
33. Schafer, R. A.; Dasler, D.; Mundloch, U.; Hauke, F.; Hirsch, A. Basic Insights into Tunable Graphene Hydrogenation. *J Am Chem Soc* **2016,** 138 (5), 1647-1652 DOI: 10.1021/jacs.5b11994.
34. Ferrari, A. C.; Meyer, J. C.; Scardaci, V.; Casiraghi, C.; Lazzeri, M.; Mauri, F.; Piscanec, S.; Jiang, D.; Novoselov, K. S.; Roth, S.; Geim, A. K. Raman spectrum of graphene and graphene layers. *Phys Rev Lett* **2006,** 97 (18), DOI: Artn 18740110.1103/Physrevlett.97.187401.
35. Graf, D.; Molitor, F.; Ensslin, K.; Stampfer, C.; Jungen, A.; Hierold, C.; Wirtz, L. Spatially resolved raman spectroscopy of single- and few-layer graphene. *Nano Lett* **2007,** 7 (2), 238-242 DOI: 10.1021/nl061702a.
36. Saikia, B. K.; Boruah, R. K.; Gogoi, P. K. A X-ray diffraction analysis on graphene layers of Assam coal. *J Chem Sci* **2009,** 121 (1), 103-106.
37. Fujimoto, H. Theoretical X-ray scattering intensity of carbons with turbostratic stacking and AB stacking structures. *Carbon* **2003,** 41 (8), 1585-1592 DOI: 10.1016/S0008-6223(03)00116-7.
38. Zeng, H. L.; Gao, C.; Yan, D. Y. Poly(epsilon-caprolactone)-functionalized carbon nanotubes and their biodegradation properties. *Adv Funct Mater* **2006,** 16 (6), 812-818 DOI: 10.1002/adfm.200500607.
39. Chadwick, R. C.; Khan, U.; Coleman, J. N.; Adronov, A. Polymer Grafting to Single-Walled Carbon Nanotubes: Effect of Chain Length on Solubility, Graft Density and Mechanical Properties of Macroscopic Structures. *Small* **2013,** 9 (4), 552-560 DOI: 10.1002/smll.201201683.
40. Degennes, P. G. Conformations of Polymers Attached to an Interface. *Macromolecules* **1980,** 13 (5), 1069-1075 DOI: Doi 10.1021/Ma60077a009.

575 For table of contents use only

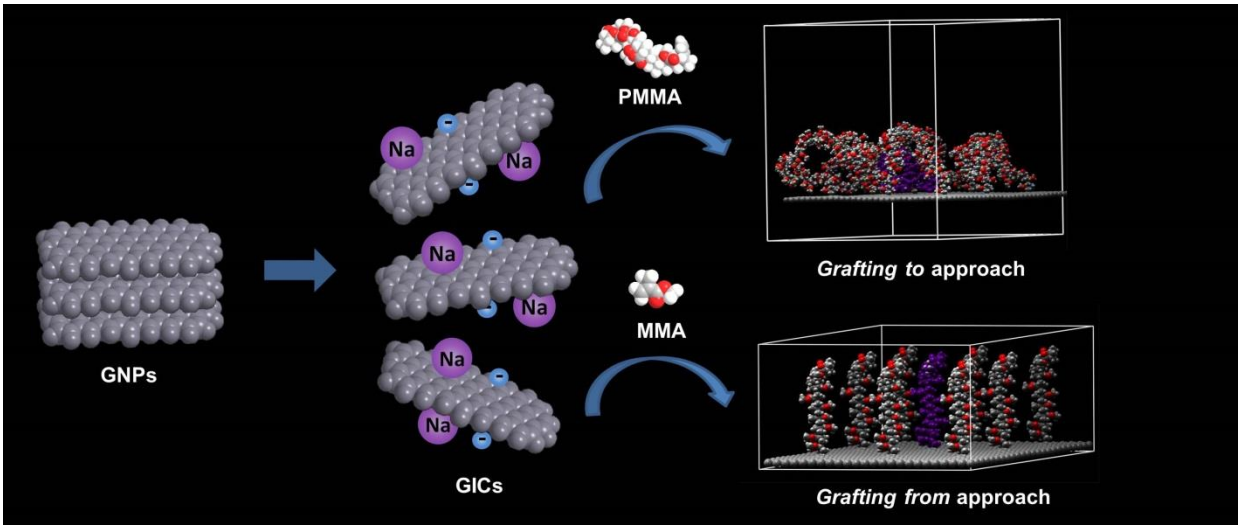

576

577

578